Proceedings of the 2019 Hypervelocity Impact Symposium
HVIS2019
April 14-19, 2019, Destin, FL, USA
HVIS2019-078

AN ACCURATE SPH SCHEME FOR HYPERVELOCITY IMPACT MODELING

Anthony Collé[a,b]* , Jérôme Limido[a] , Thomas Unfer[a] and Jean-Paul Vila[b]

[a]*Impetus AFEA, 6 rue du Cers, 31330 Grenade sur Garonne, France*
[b]*Institut de Mathématiques de Toulouse, Institut National des Sciences Appliquées de Toulouse, 135 Avenue de Rangueil, 31400 Toulouse, France*

Abstract

We focus in this paper on the use of a meshless numerical method called Smooth Particle Hydrodynamics (SPH), to solve fragmentation issues as Hyper Velocity Impact (HVI). Contrary to classical grid-based methods, SPH does not need any opening criteria which makes it naturally well suited to handle material failure. Nevertheless, SPH schemes suffer from well-known instabilities questioning their accuracy and activating nonphysical processes as numerical fragmentation. Many stabilizing tools are available in the literature based for instance on dissipative terms, artificial repulsive forces, stress points or Particle Shifting Techniques (PST). However, they either raise conservation and consistency issues, or drastically increase the computation times. It limits then their effectiveness as well as their industrial application. To achieve robust and consistent stabilization, we propose an alternative scheme called γ -SPH-ALE. Firstly implemented to solve Monophasic Barotropic flows, it is secondly extended to the solid dynamics. Particularly, based on the ALE framework, its governing equations include advective terms allowing an arbitrary description of motion. Thus, in addition of accounting for a stabilizing low-Mach scheme, a PST is implemented through the arbitrary transport velocity field, the asset of ALE formulations. Through a nonlinear stability analysis, CFL-like conditions are formulated ensuring the scheme conservativity, robustness, stability and consistency. Besides, stability intervals are defined for the scheme parameters determining entirely the stability field. Its implementation on several test cases reveals particularly that the proposed scheme faithfully reproduces the strain localization in adiabatic shear bands, a precursor to failure. By preventing spurious oscillations in elastic waves and correcting the so-called tensile instability, it increases both stability and accuracy with respect to classical approaches.

Keywords: Smoothed Particle Hydrodynamics; Arbitrary Lagrangian Eulerian; Non-Linear Stability; Tensile Instability; Strain Localization;

Nomenclature

h, Δx, $\boldsymbol{x}$	smoothing length and particle spacing and position (m)
$\boldsymbol{v}, \boldsymbol{v}_0, \boldsymbol{w}$	material velocity, arbitrary transport velocity field and relative ALE velocity (m/s)
e	specific internal energy ($\frac{\mathrm{J}}{\mathrm{kg}}$)
W, $\boldsymbol{\nabla} W, \boldsymbol{A}$	Kernel function, kernel function gradient and renormalized kernel function gradient (m^{-4})
Greek symbols	
ρ, ω	density ($\frac{\mathrm{kg}}{\mathrm{m}^3}$) and volume ($\mathrm{m}^3$)
$\boldsymbol{\Phi}$	vector of the conserved variables in $\mathbb{R}^4$
α, γ	artificial viscosity and low-Mach scheme parameters
Subscripts	
i, j	defines particles among the particle domain P
Superscripts	
k, l	defines the coordinate among *x,y,z* axis

* Corresponding author. Tel.: +33 5 61 74 86 82.
E-mail address: anthony@impetus.fr.

1. Introduction

In Aeronautics, Defense and Space, the dynamic fragmentation is induced by extreme loadings involved in events like Hypervelocity Impacts (HVI). Regarding the experimental limitations to replicate the real impact configurations, numerical tools are then crucial to study structures vulnerability. However, combining large deformations as well as numerous interface productions, this mechanism is particularly challenging from a numerical point of view. Lagrangian finite element methods (FE) are classically used to handle the numerical modeling of these events. They propose to reproduce the material failure process thanks to mesh opening techniques as element erosion, node splitting or XFEM. However, these approaches induce very long computation times. Indeed, it is due to the large number of elements needed to limit the mass lost through erosion, or to the complexity of the opening algorithms. Moreover, they experience severe energy conservation issues, whereas it is crucial in this framework. Among the Lagrangian approaches the meshless methods appear as a relevant alternative to prevent such shortcomings. We focus in this paper on the meshless method called Smooth Particle Hydrodynamics (SPH).

SPH is a Lagrangian particle method used to solve partial differential equations (PDE). Originally developed by Lucy [1] for astrophysical problems and by Gingold & Monaghan [2-4] for hydrodynamic applications (incompressible free surface flows), the method was then adapted by Libersky & Petschek [5] and Benz [6,7] to the solid mechanics by including material models. The computational domain is discretized in a set of interpolation points interpreted as particles interacting between themselves through kernel functions and carrying material properties. Based on a set of moving interpolation points then, it disregards any connectivity between its elements. Thus, it does not need any opening criteria which makes it naturally well suited to handle material failure. In addition of its conceptual simplicity, robustness, ability to handle large arbitrary deformations, to not produce diffusive interfaces and for its monolithic nature, SPH is particularly attractive. Still, SPH schemes suffer from well-known instabilities as lack of interpolation completeness, nonphysical oscillations, tensile instability or particle clumping. Questioning their accuracy, they also activate nonphysical processes as numerical fragmentation. Since its emergence, SPH benefits from many researches aiming to improve its accuracy. Thus, various stabilizing tools are available in the literature based for instance on high order kernels [8-10], additional diffusive terms [2,11,12], artificial repulsive forces [13,14] or Particle Shifting Techniques (PST) [15-18]. However, they also either raise conservation and consistency issues, or drastically increase the computation times. Thus, even if today most of the commercial transient dynamic software propose SPH like methods, its instabilities as well as its long computation times still limit its industrial application.

To achieve robust and consistent stabilization, we focus on a different SPH framework introduced by Vila [19] based on Arbitrary Lagrangian Eulerian (ALE) considerations. The idea is to combine and benefit from both Eulerian and Lagrangian movement descriptions. Indeed, the Eulerian description is generally preferred to handle large deformations, while a Lagrangian one for interface tracking. In practice this combination relies on an arbitrary transport velocity field $\boldsymbol{v}_0$, which by a smart choice, allows to increase the stability and robustness of the scheme without degrading its consistency. Generally combined to Riemann Solvers (RSALE) [17], such formulation improves the scheme accuracy, but at the cost of an increased solving complexity (solving algorithm) and low-Mach limitations [20,21]. Regarding this late aspect, in the Finite Volume (FV) framework some authors [22,23] proposed a stabilizing Low-Mach scheme. It relies on a corrective velocity term added to the continuity and momentum equations. A non-linear stability analysis provided them stability conditions (CFL-like) insuring robust and accurate computations whichever flow regime. Clayer et al. [24] adapted this Low-Mach scheme to the SPH framework and achieved similar convincing conclusions.

We propose in this work an alternative scheme called γ-SPH-ALE relying on the combination of the SPH-ALE formalism and the FV low-Mach scheme. Its governing equations and the corresponding stability conditions are exposed in section 2. Firstly, detailed for a hydrodynamic version, they are extended then to a solid formulation. Finally, in section 3, the proposed γ-SPH-ALE scheme is evaluated through several validation cases (both hydrodynamic and solid).

2. γ-SPH-ALE: A new meshless scheme

In this section the proposed γ-SPH-ALE scheme is detailed. The general SPH framework is firstly exposed and secondly apply to the ALE context. The governing equations of the proposed scheme and the corresponding stability conditions are thirdly exposed in the hydrodynamic version. They are then extended to a solid formulation.

Note that in the following Ω denotes the whole material domain, P defines the particle domain among which i describes one particle. We set V_i its neighboring particle set, and we take $j \in V_i$. Finally, $n \in \mathbb{N}$ defines the time step number and $d \in \mathbb{N}^*$ the space dimension. In this section we refer to [19,25] for more details on SPH and SPH-ALE.

2.1. SPH basics

SPH relies on approximation features allowing to discretize conservation laws on a particle set $(x_i, \omega_i)_{i\in P}$ (respectively the particle position and volume). These approximations are achieved thanks to kernel functions $W(\|\boldsymbol{x}_i - \boldsymbol{x}_j\|, h) = W_{ij}$ depending on the smoothing length h (half radius of its compact support) and the distance between two particles. The kernel gradient can also be evaluated as $\boldsymbol{\nabla} W_{ij} = grad_x W_{ij}$ allowing to define then the smoothed particle approximation of a function f and of its derivative

$$\Pi^h(f)_i = \sum_{j\in P} \omega_j\, f_j W_{ij} \ \text{ and } \ \boldsymbol{\nabla}\Pi^h(f)_i = \sum_{j\in P} \omega_j\, f_j \boldsymbol{\nabla} W_{ij} \tag{1}$$

As introduced above, classical SPH suffers from a lack of interpolation completeness which can be compensated by using renormalized kernels. Vila [9] proposed to replace $\boldsymbol{\nabla} W_{ij}$ by $\boldsymbol{A}_{ij} = B_{ij}\boldsymbol{\nabla} W_{ij}$ where $\boldsymbol{B}_{ij} = (\boldsymbol{B}_i + \boldsymbol{B}_j)/2$ and B is the renormalization matrix (introduced by Johnson et al. [8] and Vila [9]) defined as

$$B_i = E_i^{-1} \ \text{ and } \forall (k,l) \in [\![1,..,d]\!]^2, E_i^{kl} = \sum_{j\in P} \omega_j \left(\boldsymbol{x}_j^l - \boldsymbol{x}_i^l\right)\boldsymbol{\nabla} W_{ij}^k \tag{2}$$

We set in the following $\boldsymbol{n}_{ij} = \boldsymbol{A}_{ij}/\|\boldsymbol{A}_{ij}\|$.

To ensure the conservative property of the scheme, alternative derivative operators are used in practice and combined to symmetric kernels such that $W_{ij} = W_{ji}$ and $\boldsymbol{\nabla} W_{ij} = -\boldsymbol{\nabla} W_{ji}$

$$\boldsymbol{D_h} f_i = \sum_{j\in P} \omega_j \left(f_j - f_i\right)\boldsymbol{A}_{ij} \ \text{ and } \ \boldsymbol{D}_h^* f_i = \sum_{j\in P} \omega_j \left(f_j + f_i\right)\boldsymbol{A}_{ij} \tag{3}$$

Note that, as proved in [19], operator $\mathbf{D}_{\boldsymbol{h}}$ (3) combined to renormalization strongly approximates the gradient operator under the condition $\Delta x/h = O(1)$ (where Δx is the particle spacing). It is a crucial point to ensure the scheme consistency. In standard SPH this convergence property depends on the ratio $\Delta x/h$ and is only enforced for particular values [22]. Classically $h = 1.3\Delta x$ in 3D.

2.2. ALE Framework

The idea is now to apply these approximation features to a conservation law in ALE formalism. We consider then the following law

$$L_{v0}(\boldsymbol{\Phi}) + div[F_E(\boldsymbol{\Phi}) - \boldsymbol{\Phi}\otimes\boldsymbol{v}_0] = S(\boldsymbol{\Phi}) \ \text{ with } \ L_v\colon \boldsymbol{\Phi} \to \frac{\partial \boldsymbol{\Phi}}{\partial t} + \sum_{k=1,..,d}\frac{\partial(v^k\boldsymbol{\Phi})}{\partial x^k} \tag{4}$$

Where $\boldsymbol{v}_0 \in \mathbb{R}^3$ is a regular transport field, $\boldsymbol{\Phi} \in \mathbb{R}^4$ the vector of the conserved variables, $\boldsymbol{F}_E = (F_E^k)_k^4$ the Eulerian flux vectors, $\boldsymbol{S} = (S^k)_k^4$ the source term and L_{v0} the transport operator associated to $\boldsymbol{v}_0$. Considering the continuum mechanics equations, we have

$$\boldsymbol{\Phi} = \begin{pmatrix}\rho\\ \rho\boldsymbol{v}\\ \rho e\end{pmatrix}, \boldsymbol{F}_E = \begin{pmatrix}\rho\boldsymbol{v}\\ -\boldsymbol{\sigma} + \rho\boldsymbol{v}\otimes\boldsymbol{v}\\ -\boldsymbol{\sigma}.\boldsymbol{v} + \rho e\boldsymbol{v}\end{pmatrix} \text{ and } \boldsymbol{S} = \begin{pmatrix}0\\ \rho\boldsymbol{f}\\ \rho\boldsymbol{f}.\boldsymbol{v}\end{pmatrix} \tag{5}$$

Where $\rho, \boldsymbol{v}, e$ and $\boldsymbol{\sigma}$ are respectively the density, material velocity, specific total energy and stress tensor. Thus, to approximate (4) considering the moving particle set $(x_i, \omega_i)_{i\in P}$, we apply the SPH discretization process detailed in [19] based on the weak formulation of (4) providing the following equation

$$\frac{d(\omega_i \boldsymbol{\Phi}_i)}{dt} + \omega_i \sum_{k=1,..,d} \boldsymbol{\nabla}_h^{k,*} [F_E^k(\boldsymbol{\Phi}) - \boldsymbol{v}_0^k . \boldsymbol{\Phi}] = 0 \quad (6)$$

Where $-\boldsymbol{\nabla}_h^*$ is the dual of an operator $\boldsymbol{\nabla}_\mathrm{h}$ approximating the derivative operator $\boldsymbol{\nabla}$.

2.3. Application to the Barotropic Euler Equations

The idea is to choose $\boldsymbol{\nabla}_\mathrm{h}$ in order to stay conservative and consistent. Several choices are admissible (as $\mathbf{D}_{\boldsymbol{h}}$ (3) like in [19]), and we propose to work with the following scheme discretized in space

$$\frac{d\boldsymbol{x}_i}{dt} = \boldsymbol{v}_{0i} \quad (7)$$

$$\frac{d\omega_i}{dt} = \omega_i \sum_{j\in P} \omega_j \left\langle \left(\boldsymbol{v}_{0j} - \boldsymbol{v}_{0i}\right), \boldsymbol{A}_{ij} \right\rangle \quad (8)$$

$$\frac{d(\omega_i \rho_i)}{dt} = -\omega_i \sum_{j\in P} \omega_j \left(\rho_j + \rho_i\right) \langle \boldsymbol{w}_{ij}, \boldsymbol{A}_{ij} \rangle \quad (9)$$

$$\frac{d(\omega_i \rho_i \boldsymbol{v}_i)}{dt} = -\omega_i \sum_{j\in P} \omega_j \left[\left(\rho_j \boldsymbol{v}_j + \rho_i \boldsymbol{v}_i\right) \langle \boldsymbol{w}_{ij}, \boldsymbol{A}_{ij} \rangle + p_{ij} \boldsymbol{A}_{ij} - \boldsymbol{\pi}_{ij} \right] \quad (10)$$

With

$$\boldsymbol{w}_{ij} = \frac{1}{2}\left(\boldsymbol{w}_i + \boldsymbol{w}_j\right) - \boldsymbol{\Gamma}_{ij} \quad (11)$$

$\boldsymbol{w}$ corresponds to the relative ALE velocity defined by $\boldsymbol{w} = \boldsymbol{v} - \boldsymbol{v}_0$. We also define $p_{ij} = p_i + p_j$, $\boldsymbol{\Gamma}_{ij}$ corresponds to the stabilizing term coming from the FV low-Mach scheme and $\boldsymbol{\pi}_{ij}$ corresponds to the artificial viscosity. $\langle .,. \rangle$ defines the usual scalar product on $\mathbb{R}^d$.

A vectorial version of Monaghan's stabilizing artificial viscosity [2] is proposed. It depends on a parameter α to adjust in order to minimize the amount of artificial diffusion induced in the scheme. c_0 is the material sound speed and $\rho_{ij} = \left(\rho_i + \rho_j\right)/2$

$$\boldsymbol{\pi}_{ij} = \alpha_{ij}\left(\boldsymbol{v}_j - \boldsymbol{v}_i\right) \text{ with } \alpha_{ij} = \alpha c_0 \rho_{ij} \left\| \boldsymbol{A}_{ij} \right\| \quad (12)$$

The coupling between the SPH version of the FV Low-Mach scheme and the SPH-ALE formalism is achieved by the term $\boldsymbol{\Gamma}_{ij}$ through the mean relative ALE velocity $\boldsymbol{w}_{ij}$

$$\boldsymbol{\Gamma}_{ij} = \gamma_{ij}\left(p_j - p_i\right)\boldsymbol{n}_{ij} \text{ with } \gamma_{ij} = \frac{\gamma}{2c_0\rho_{ij}} \quad (13)$$

Note that, according to (7-10) the choice of γ is totally independent from the choice of the movement description (meaning from the choice of $\boldsymbol{v}_0$). Also disregarding $\boldsymbol{\Gamma}_{ij}$ and $\boldsymbol{\pi}_{ij}$, the classical Lagrangian SPH formulation ($\boldsymbol{w} = \boldsymbol{0}$) with constant masses $m_i = \omega_i \rho_i$ is recovered. With this ALE formulation particles are moved following the velocity field $\boldsymbol{v}_0$ (7). Such field is said to be arbitrary in the sense that, as suggested by Vila [19], a smart choice of $\boldsymbol{v}_0$ could increase both stability and robustness of the calculations without its consistency. Various methods are available in the literature as Monaghan's XSPH method [3] or PST [15-18]. They consist in reorganizing the particle set during calculations (quasi-lagrangian mode) to prevent instabilities such as tensile instability [13] or the formation of Lagrangian particle structures [16]. The idea is to set $\boldsymbol{v}_{0i} = \boldsymbol{v}_i + \boldsymbol{\delta v}_i$ where $\boldsymbol{\delta v}_i$ stores the regularizing technique. The integration is performed thanks to a second order Runge-Kutta Heun (RK2H) time integration scheme defined as

$$\begin{cases} \overline{\boldsymbol{\Theta}}^{n+1} = \boldsymbol{\Theta}^n + \Delta t \dfrac{d\boldsymbol{\Theta}^n}{dt} \\ \boldsymbol{\Theta}^{n+1} = \dfrac{1}{2}\left[\boldsymbol{\Theta}^n + \overline{\boldsymbol{\Theta}}^n + \Delta t \dfrac{d\overline{\boldsymbol{\Theta}}^{n+1}}{dt}\right] \end{cases} \text{ Where } \boldsymbol{\Theta} = (\boldsymbol{x}, \omega, \omega\rho, \omega\rho\boldsymbol{v})^t \quad (14)$$

2.4. Nonlinear Stability Analysis

In order to ensure that the proposed scheme is conservative, robust, stable and consistent, stability conditions on the scheme parameters are exhibited thanks to a nonlinear stability analysis. The proof is briefly presented but not detailed in this paper, we refer to the work of Grenier et al. [22], Lavalle et al. [23] and Couderc et al. [26] for a similar process in a FV framework.

According to the equation set (7-10), and considering that $\boldsymbol{A}_{ij} = -\boldsymbol{A}_{ji}$, $\boldsymbol{w}_{ij} = \boldsymbol{w}_{ji}$ (11,13) and $\boldsymbol{\pi}_{ij} = -\boldsymbol{\pi}_{ji}$ (12) we can show that the proposed scheme is indeed conservative. Also, according to (8) the volume evolution is controlled by the imposed field $\boldsymbol{v}_0$ which provides volume bounds $(\omega_{min}, \omega_{max}) \in \mathbb{R}^{+*}$. Now, thanks to (9), and considering $(\omega_{min}, \omega_{max})$, we can find a CFL $N_\rho \in \mathbb{R}^{+*}$ which, insures the existence of density bounds $(\rho_{min}, \rho_{max}) \in \mathbb{R}^{+*}$ and achieves the expected robustness. Regarding the scheme stability, an energy balance is performed. The idea is to provide a CFL condition ensuring a control on the system total energy $\mathcal{E}$. We define $\mathcal{E} = \frac{1}{2}\rho\|\boldsymbol{v}\|^2 + \varphi$ where $\varphi = \rho \int_{\rho_0}^{\rho} \frac{p(r)}{r^2} dr$ is the total free energy and corresponds to the barotropic pressure. Through this energy balance, the production terms are exhibited and evaluated. It allows to highlight a CFL $N_E \in \mathbb{R}^{+*}$ insuring that

$$\begin{gathered} For\ \frac{\Delta t c_0}{h} \leq N_E,\ \exists \mathcal{E}_T \in \mathbb{R}^{+*}, \exists(\alpha_{min}, \alpha_{max}, \gamma_{min}, \gamma_{max}) \in \mathbb{R}^{+,4}\ such\ that \\ \forall(\alpha, \gamma) \in [\alpha_{min}, \alpha_{max}]x[\gamma_{min}, \gamma_{max}], \forall t \in [0, T], \mathcal{E}(t) \leq \mathcal{E}_T \end{gathered} \tag{15}$$

It worth noticing that these stability conditions are defined regardless the expression of $\boldsymbol{v}_0$ revealing its arbitrary property previously introduced. However, they still depend on a geometrical constant meaning that the stability is ensured while the particle distribution stays regular enough. Then it is crucial to be allowed to implement a conservative and consistent regularizing technique through $\boldsymbol{v}_0$ such as PST. Considering now the volume, density and energy bounds (15), we can finally achieve the weak consistency of the proposed scheme thanks to a Lax-Wendroff like theorem. We refer to [19] where Vila details the employed technique.

2.5. Extension to Solids dynamics

The proposed γ-SPH-ALE scheme is then directly extended to account for material strength. To do so the momentum equation (10) is enhanced by the deviatoric stress tensor contribution. To account for material strength models, we use then discrete formulations of strains, to describe the isotropic linear elasticity (through Hooke's law), and rotation, to insure the stresses objectivity (through Jaumann's derivative). Working in an ALE framework, a discretization of the advection component of path-dependent variables, such as stresses, is also considered. Thanks to the Von Mises yield stress criterion and a flow stress model, we are then able to describe the material plastic flow. Aiming to handle the fragmentation process, we also consider a description of the material damage growth, a direct consequence of its deformation and a precursor to its failure. Finally, we implement an initial damage distribution as well to account for material heterogeneity determining its failure behavior (presence of structural defects such as inclusions or cavities). See [18,27] for similar detailed processes.

3. Validation

In order to evaluate the capability of γ-SPH-ALE, we propose to investigate three test cases: isentropic shock tube, cylinder fragmentation and hypervelocity impact.

3.1. Isentropic Shock Tube

The isentropic shock tube is a classical academic test case with a known exact solution. Many configurations and data are available in the literature allowing then to efficiently evaluate γ-SPH-ALE. We focus here on a simple barotropic shock tube using a linear equation of state (EOS) (21). We choose the case of a pressure discontinuity generated by the following initial density field (22,23) (where L and R define the left and right states).

$$p = c_0^2(\rho - \rho_0)\ and\ \begin{cases} \rho_L = 1100\ kg/m^3\ and\ \|\boldsymbol{v}_L\| = 0\ m/s \\ \rho_R = 1000\ kg/m^3\ and\ \|\boldsymbol{v}_R\| = 0\ m/s \end{cases} \tag{16}$$

The fluid is taken as having a referential density ρ_0=1000kg/m3 and a sound speed c_0=1466m/s. The tube is taken with a length *Lx*=0.1m and a width *Ly*=0.01m. The discontinuity is initially defined at *x*=0.05m. All computations are performed with cubic B-splines kernel functions and a fixed smoothing length. The exact solution used as a reference is given by an exact 1D Riemann solver with 2000 cells. SPH computations are performed in 2D with periodic boundary conditions to mimic a 1D case. We present the results given by standard SPH (with Monaghan's artificial viscosity such as α=β=1.5), by an ALE SPH HLLC Riemann solver with a MUSCL scheme (RSALE), and by the γ-SPH-ALE scheme (used with *α*=0.0). The initial spacing is set to *Δx*=2.10-4m, giving 50.000 particles. Note that for standard SPH the values of the artificial viscosity parameters correspond to a threshold below which the scheme is unstable (significant overshoots).

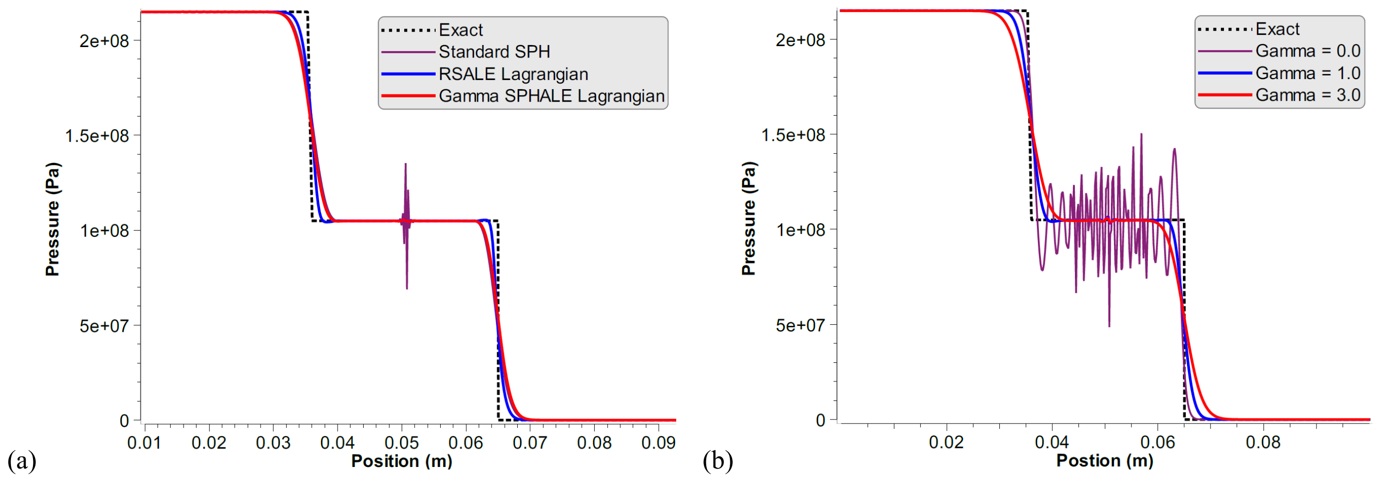

Fig. 1. **Shock Tube** Pressure fields comparisons at $t = 10^{-5}s$ (a) for several schemes (*γ*=1.0 for Gamma SPHALE), (b) for γ-SPH-ALE with several values of γ.

As depicted on Fig.1a the discontinuity generates a left rarefaction wave and a right shock wave. The solution is then characterized by three pressure levels (2.14928 Pa, 1.04938 Pa, 0 Pa). Fig. 1a shows the comparison between the exact solution, standard SPH, RSALE and γ-SPH-ALE with *γ*=1.0. Standard SPH, RSALE and γ-SPH-ALE are all able to reproduce the pressure jumps. While capturing correctly the pressure jumps, standard SPH produces significant oscillations at the discontinuity initial position both RSALE and γ-SPH-ALE manage to prevent. Note that these oscillations cannot be prevented even with more artificial viscosity. Also, RSALE manages to capture the jumps more efficiently than standard SPH and γ-SPH-ALE, generating narrower pressure variations. However, RSALE also produces overshoots the proposed scheme completely damps.

Regarding the choice of γ, Fig. 1a results are obtained with the value corresponding to the threshold below which overshoots appear. Fig. 1b shows the results for different γ. We can see that increasing its value stabilizes the scheme by damping the oscillations in a very efficient way, but it also diffuses the shocks (larger jumps). γ-SPH-ALE is then able to faithfully reproduce the shocks and the use of γ allows to easily control its stability and accuracy without the Riemann solver complexity. Note that both RSALE and γ-SPH-ALE (for a given value of γ) produce results identical to the one presented on Fig. 1b (Lagrangian description of motion i.e. $\boldsymbol{v}_0 = 0$) in Eulerian description of motion ($\boldsymbol{v}_0 = 0$) or with PST (ALE description of motion i.e. $\boldsymbol{v}_0 = arbitrary$).

3.2. Hypervelocity Impact

Hypervelocity Impacts are events occurring at velocities around 1 to 10 km/s. They are particularly challenging for space vehicles design when generated by orbiting debris. Regarding the experimental limitations (to reach the impact velocity), providing reliable predictive modelling is then crucial to evaluate the vehicle vulnerability. We focus here on the case of an Aluminium sphere (diameter 9.53 mm) impacting Aluminium plates with different thickness at 6.7 km/s. The experiment is described in [26]. Two cases are reproduced: 1- thickness = 0.8 mm, 2- thickness = 4.039 mm. The γ-SPH-ALE scheme is implemented in full 3D with an Elastic perfectly Plastic material model as well as a Mie-Gruneisen equation of state. The spalling process is managed by a pressure threshold above which the deviatoric stress is relaxed (only pressure remains). Such simple criterion is used as the idea is to evaluate the γ-SPH-ALE scheme ability to reproduce the cloud of debris. The constitutive parameters are the following: ρ_0 = 2703 kg/m3, Young modulus 76 GPa, Poisson ratio 0.3, Yield stress 260 MPa, Linear Hugoniot Slope coefficient 1.338, Gruneisen gamma 2.0. The numerical results are achieved with $1{,}5.\,10^6$ SPH particles.

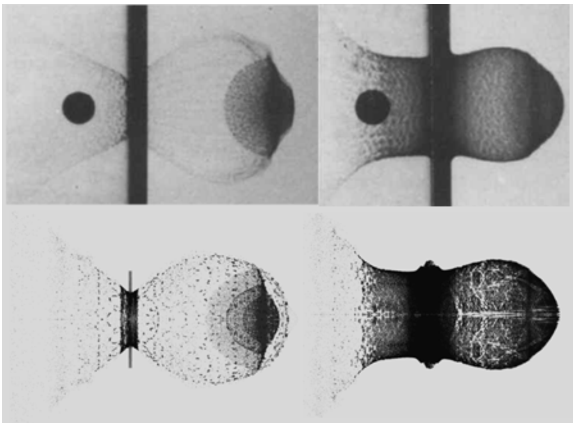

(a)

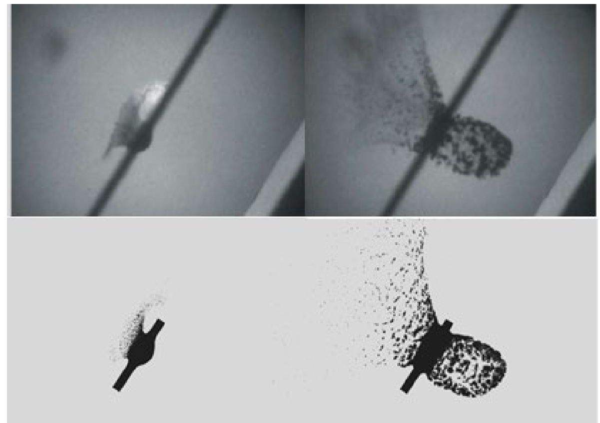

(b)

Fig. 2. **Hypervelocity Impact** Comparison between experiments (top) and γ-SPH-ALE (bottom) (a) normal impact Thickness = 0.8mm (left), Thickness = 4.039 mm (right), (b) oblique impact.

Fig. 2a shows the experimental and numerical results for both configurations described above. The experimental results are achieved thanks to X-ray flashes. We can see that in both configurations the numerical model is able to faithfully reproduce the cloud of debris characteristic features: an ejecta veil on the plate front side, an expending debris cloud "bubble" on the plate rear side and a disc-like structure inside the expending bubble (appearing clearly on case thickness 0.8 mm).

A similar configuration is now studied and corresponds to an oblique HVI. The sphere diameter is 3 mm with a velocity 4050 m/s and the plate thickness is 2 mm. Both elements still are in Aluminium (same constitutive parameters). However, the plate is now 32° tilted with respect to the sphere impact direction. Fig. 2b-top shows the experimental results at different times achieved by Thiot Ingenerie (introduced in [29]), and Fig. 2b-bottom shows the γ-SPH-ALE numerical results full 3D with $6{,}5.\,10^6$SPH particles. We can see that the proposed numerical model is again able to faithfully reproduce the cloud of debris shape.

4. Conclusion

We have proposed a new mesh-less scheme called γ-SPH-ALE based on the combination of both SPH-ALE formulation [14] and FV low-Mach scheme [19,20]. PDE are written in ALE formalism (4) allowing for a simple treatment of the arbitrary velocity field $\boldsymbol{v}_0$, ruling the particle motion (7). A stabilizing term extracted from the FV low-Mach scheme is also introduced by means of a velocity corrective term (11,13) (depending on a parameter γ). Proportional to the pressure gradient it improves the state variables evaluation. An artificial viscosity (12) (depending on a parameter α) is combined with this γ velocity to ensure the global stability of the scheme. The arbitrary property of $\boldsymbol{v}_0$ also allows to implement a PST increasing both accuracy and stability while maintaining the conservative and consistency property of the scheme.

We evaluated the performances of the γ-SPH-ALE scheme (for both hydrodynamic and solid contexts) on two test cases: isentropic shock tube and hypervelocity impact. For the shock tube case the γ-SPH-ALE scheme managed to faithfully reproduce the pressure field by efficiently damping the spurious oscillations (in both Lagrangian and Eulerian descriptions). Regarding the HVI cases, γ-SPH-ALE managed to faithfully reproduce the cloud of debris for both normal and oblique configurations.

Future works will be the enhancement of material models and fracture modelling to handle more complex materials and configurations.

Acknowledgements

We want to firstly thank the Institut de Mathématiques de Toulouse, the Institut National des Sciences Appliquées de Toulouse as well as the Université Paul Sabatier for providing the necessary literature resources to conduct the researches through online review access. Besides, we also thank particularly Impetus AFEA for providing the numerical material needed for the investigations (workstations with Impetus Solver®).

References

[1] Lucy, L. B., 1977. A numerical approach to the testing of the fission hypothesis, Astronomical Journal 82, p. 1013-1024.
[2] Monaghan, J., Ginglod, R. A.,1983. Shock Simulation by the Particle Method SPH. Journal of Computational Physics 52, p. 374-389.
[3] Monaghan, J., 1992. Smoothed Particle Hydrodynamics, Annual review of astronomy and astrophysics 30, p.543-574.
[4] Monaghan, J., 1994. Simulating Free Surface Flows with SPH. Journal of Computational Physics 110, p. 399-406.
[5] Libersky, L.D. and Petschek, A.G., 1991. Smooth particle hydrodynamics with strength of materials, in *"Advances in the Free-Lagrange Method Including Contributions on Adaptive Gridding and the Smooth Particle Hydrodynamics Method"* Trease, H.E. and Fritts, M.F. and Crowley, W.P. Editor. Lecture Notes in Physics, Berlin Springer Verlag, vol. 395, p. 248-257.
[6] Benz, W., 1990. Smooth Particle Hydrodynamics: A Review. The Numerical Modelling of Nonlinear Stellar Pulsations, p. 269-288.
[7] Benz, W., Asphaug, E., 1994. Impact Simulations with Fracture. I. Method and Tests. Icarus 107, p. 98-116.
[8] Johnson, G. R., Beissel, S. R., 1996. Normalized Smoothing Functions for SPH Impact Computations. International Journal for Numerical Methods in Engineering 39, p. 2725-2741.
[9] Vila, J. P., 1998. "Methodes particulaires regularisees. Developpements recents et nouvelles applications". ESAIM Proceedings 3 p. 131-146.
[10] Frontiere, N., Raskin, C. D., Owen, J. M., 2017. CRKSPH: A Conservative Reproducing Kernel Smoothed Particle Hydrodynamics Scheme. Journal of Computational Physics 332, p. 160-209.
[11] Marrone, S., Antuono, M., Colagrossi, A., Colicchio, G., Touze, D. L., Graziani, G., 2011. Computer Methods in Applied Mechanics and Engineering 200, p. 1526-1542.
[12] Antuono, M., Colagrossi, A., Marone, S., 2012. Numerical diffusive terms in weakly-compressible SPH schemes. Computer Physics Communications 183, p. 2570-2580.
[13] Monaghan, J., 2000. SPH Without a Tensile Instability. Journal of Computational Physics 159, p. 290-311.
[14] Swegle, J., Hicks, D., Attaway, S., 1995. Smoothed Particle Hydrodynamics Stability Analysis. Journal of Computational Physics 116, p. 123-134.
[15] R. Xu, R., Stansby, P., Laurence, D., 2009. Accuracy and stability in incompressible SPH (ISPH) based on the projection method and a new approach. Journal of Computational Physics 228, p. 6703-6725.
[16] Lind, S., Xu, R., Stansby, P., Rogers, B., 2012. Journal of Computational Physics 231, p. 1499-1523.
[17] Oger, G., Marrone, S., le Touze, D., de Leffe, M., 2016. SPH Accuracy Improvement through the Combination of a Quasi-Lagrangian Shifting Transport Velocity and Consistent ALE Formalism. Journal of Computational Physics 313, p. 76-98.
[18] Zhang, C., Hu, X. Y., Adams, N. A.,2017. A generalized transport-velocity formulation for Smoothed Particle Hydrodynamics. Journal of Computational Physics 337, p. 216 – 232.
[19] Vila, J. P., 1999. On Particle Weighted Methods and Smooth Particle Hydrodynamics. Mathematical Models and Methods in Applied Sciences 09, p. 161-209.
[20] Guillard, H., Viozat, C., 1999. On the behavior of upwind schemes in the low Mach number limit. Computers and Fluids 28, p. 63-86.
[21] Degond, P., Tang, M., 2011. All Speed Scheme for the Low Mach Number Limit of the Isentropic Euler Equations. Communications in Computational Physics 10, p. 1-31.
[22] Grenier, N., Vila, J. P., Villedieu, P., 2013. An Accurate low-Mach Scheme for a Compressible Two-fluid Model Applied to Free-surface Flows. Journal of Computational Physics 252, p. 1-19.
[23] Lavalle, G., Vila, J. P., Blanchard, G., Laurent, C., Charru, F., 2015. A Numerical Reduced Model for Thin Liquid Films Sheared by a Gas Flow. Journal of Computational Physics 301, p. 119-140.
[24] Clayer, M., Lacome, J. L., Limido, J., Vila, J. P., 2014. "Pressure Evaluation Improvement for Euler Isentropic SPH Scheme", Proceedings of the 9th international SPHERIC workshop, Paris, France.
[25] Lanson, N. and Vila, J.P., 2008. Renormalized Meshfree Schemes I: Consistency, Stability, and Hybrid Methods for Conservation Laws. SIAM Journal on Numerical Analysis 46, p. 1912-1934.
[26] Couderc, F., Duran, A., Vila, J. P., 2017.An explicit asymptotic preserving low Froude scheme for the multilayer shallow water model with density stratification. Journal of Computational Physics 343, Supplement C, p. 235-270.
[27] Huerta, A., Casadei, F., 1994. New ALE applications in nonlinear fast transient solid dynamics. Engineering Computations 11, p. 317-345.
[28] Piekutowski, A. J., 1993. Characteristics of debris clouds produced by hypervelocity impact of aluminum spheres with thin aluminum plates. International Journal of Impact Engineering 14, p. 573-586.
[29] Plassard, F., Mespoulet, J., Hereil, P., 2011. "Hypervelocity impact of aluminium sphere against aluminium plate: experiment and LS-DYNA correlation", 8th European LS-DYNA Users Conference, Strasbourg, France.